A Geometric Approach for Deriving Multicontact Dynamic Identification Models

Robert Matthew
Gentiane Venture
Ruzena Bajcsy

Electrical Engineering and Computer Sciences
University of California at Berkeley

Technical Report No. UCB/EECS-2016-38
http://www.eecs.berkeley.edu/Pubs/TechRpts/2016/EECS-2016-38.html

May 1, 2016

A Geometric Approach for Deriving Multicontact Dynamic Identification Models

Robert Peter Matthew[1], Gentiane Venture[2] and Ruzena Bajcsy[1]

***Abstract*— Dynamic identification models allow for system parameters such as mass and inertia to be computed by combining knowledge of the system's configuration, and the forces applied to the system. These methods are often used to calibrate individual dynamic models in robots, and have also been used to estimate human parameters. While commonly used, the Denavit-Hartenberg approach can lead to modelling errors due to limitations in modelling rotations about arbitrary axes. This paper introduces a geometric framework for dynamic identification modelling. Geometric models rotation axes to be written explicitly, and offer a concise representation for common kinematic and dynamic operations. This Geometric approach is compared to the DH form, highlighting the ease in modelling complex rotations and the reduction in error due to the removal of oversimplification. Multiple points of contact can also be modelled easily using the geometric approach, allowing for under-actuated systems to be identified.**

I. INTRODUCTION

Dynamic models allow insight into the relation between the motion of the system and the forces applied to it. These models can be used to simulate and control a system, allowing optimal trajectories to be generated and executed. While the dynamic parameters can be estimated from the geometric structure and material properties, these models may not be accurate enough or take into account the individual variations. In these cases, dynamic identification methods are required to estimate the system dynamic properties.

Given knowledge of the joint torques and the corresponding motions, it is possible to estimate the dynamic parameters [1]. These approaches are common in robotics applications as the joint torques are often measured using sensors, or can be estimated from the motor current [2].

If the joint torques are not known, it is possible to estimate the dynamic parameters through the contact forces in the system [3]. This approach is commonly used by researchers investigating human dynamic parameters as joint torques are difficult to determine without invasive surgery [4]. Due to the variation between different individuals, and the clinical utility, these contact based models offer an opportunity to non-invasively estimate the dynamics of an individual.

One of the drawbacks of these methods is computing the *Dynamic Identification Model* (DIM) [5]. Derivation of a system DIM is often performed using Denavit-Hartenberg (DH) parameters. While these parameters are standard for robotics applications where the rotations are typically purely revolute, and the positions and axes are accurately aligned, this is not always the case. With the advent of affordable low cost robots, and the application to humans, the assumption of simple revolution about the standard Euclidean axes may not be valid. While the DH approach can be adjusted to take into account rotations about arbitrary axes, this approach can require the introduction of multiple intermediary frames.

Geometric modelling methods are an alternative to the DH approach, representing complex rotations as exponents of skew-symmetric matrices [6]. By adopting this approach, we show it is possible to obtain a fully descriptive DIMs in a compact form.

This work extends the geometric modelling approach to derive DIMs. It is divided into five main sections. After an initial overview into DIM modelling and Geometric robotics (Section III), the initial form of the geometric DIM is given (Section IV). This method is validated against the DH model for a system with rotations collinear to the standard Euclidean bases (Section V). Section VI shows the effect of oversimplifying a rotational axes. Finally, the Geometric DIM model is completed by extending it to model multiple contacts (Section VII).

II. NOTATION

$\mathbb{O}$	matrix of zeros; dimension clear from context
$\mathbb{I}$	identity matrix; dimension clear from context
$\boldsymbol{\tau}_{\boldsymbol{J}i}$	$\in \mathbb{R}$ joint torque at the i^{th} joint.
$\boldsymbol{\Gamma}_i$	$\in \mathbb{R}^{6n\times 1}$ wrench vector in the form $\left[\boldsymbol{F}_i^T, \boldsymbol{\tau}_i^T\right]^T$. $\boldsymbol{F}_i$ and $\boldsymbol{\tau}_i$ are the forces and torques acting on frame i.
$\boldsymbol{Y}$	the regressor matrix $\boldsymbol{Y}(\boldsymbol{\theta}, \dot{\boldsymbol{\theta}}, \ddot{\boldsymbol{\theta}})$ is a matrix of the kinematic structure of the system.
m_i	is the mass of segment i. It is located at the point with the coordinates $(r_{i,x}, r_{i,y}, r_{i,z})$.
$\boldsymbol{I}$	$\in \mathbb{R}^{3\times 3}$ is a moment of inertia about the center of mass. The elements of $\boldsymbol{I}$ are written I_{xx}, I_{yy} etc.
$\boldsymbol{\phi}_i$	$= \begin{bmatrix} m_i & m_i r_{i,x} & m_i r_{i,y} & m_i r_{i,z} & I_{i,xx} \\ I_{i,yy} & I_{i,zz} & I_{i,xy} & I_{i,xz} & I_{i,yz} \end{bmatrix}^T$
$\boldsymbol{\phi}$	$= \begin{bmatrix}\boldsymbol{\phi}_1^T & \dots & \boldsymbol{\phi}_n^T\end{bmatrix}^T$
$\boldsymbol{\psi}$	are the subset of $\boldsymbol{\phi}$ that are identifiable. These are known as the *base parameters*.
$\boldsymbol{\omega}^b$	$\in \mathbb{R}^{3\times 1}$ is a unit vector denoting the axis of rotation, viewed in the body frame.
$\boldsymbol{v}^b$	$\in \mathbb{R}^{3\times 1}$ is a unit vector denoting the direction the origin of the body frame relative to the spatial frame, viewed in the body frame.

*This work was supported by NSF grant 1354321 and JSPS Grant-in-Aid for Young Scientists K125870209

[1]Electrical Engineering and Computer Science, University of California at Berkeley, USA. {rpmatthew, bajcsy} @berkeley.edu
[2]Department. of Mechanical Systems Engineering, Tokyo University of Agriculture & Technology, Tokyo, Japan

III. BACKGROUND

A. Dynamic Identification Models

The dynamics of a serial chain structure can be represented by the expression:

$$\boldsymbol{H}\begin{bmatrix}\ddot{\boldsymbol{q}}_0\\ \ddot{\boldsymbol{\theta}}\end{bmatrix}+\boldsymbol{b}=\begin{bmatrix}\mathbb{O}\\ \boldsymbol{\tau}_J\end{bmatrix}+\sum_{k=1}^{N_c}\begin{bmatrix}\boldsymbol{K}_{k1}\\ \boldsymbol{K}_{k2}\end{bmatrix}\boldsymbol{\Gamma}_k \tag{1}$$

where $\boldsymbol{\Gamma}_k$ are the contact forces acting on the chain [5]. By combining the inertial matrix ($\boldsymbol{H}$) and the centrifugal, Coriolis and gravity forces ($\boldsymbol{b}$), it is possible to rearrange the expression for the dynamics into:

$$\begin{bmatrix}\boldsymbol{Y}_{T1}\\ \boldsymbol{Y}_{T2}\end{bmatrix}\boldsymbol{\phi}=\begin{bmatrix}\mathbb{O}\\ \boldsymbol{\tau}_J\end{bmatrix}+\sum_{k=1}^{N_c}\begin{bmatrix}\boldsymbol{K}_{k1}\\ \boldsymbol{K}_{k2}\end{bmatrix}\boldsymbol{\Gamma}_k \tag{2}$$

where the regressor ($\boldsymbol{Y}_T$) relates the full dynamic parameters ($\boldsymbol{\phi}$) to the forces ($\boldsymbol{F}_k$) and torques ($\boldsymbol{\tau}$) acting on the system. In systems where the joint torques are not typically available (such as in biological systems), the system dynamics that can be decoupled from the joint torques:

$$\boldsymbol{Y}_{T1}\boldsymbol{\phi}=\sum_{k=1}^{N_c}\boldsymbol{K}_{k1}\boldsymbol{\Gamma}_k \tag{3}$$

Equation 3, can be used to recover the full dynamic parameters ($\boldsymbol{\phi}$), provided $\boldsymbol{Y}_{T1}$ is invertible. The invertibility of $\boldsymbol{Y}_{T1}$ is rare, preventing the recovery of ($\boldsymbol{\phi}$).

To overcome this obstacle, the invertible parts of $\boldsymbol{Y}_{T1}$ can be found (typically using the QR decomposition) resulting in the base regressor $\boldsymbol{Y}_b$ [7]. This allows for parameters to be combined and removed based on the linear dependency of the system. The dynamic parameters that are recoverable can therefore be written as the base parameters $\boldsymbol{\psi}$ where:

$$\boldsymbol{Y}_b\boldsymbol{\psi}=\sum_{k=1}^{N_c}\boldsymbol{K}_{k1}\boldsymbol{\Gamma}_k \tag{4}$$

To validate this process, two checks are often used. The first is a measure of the invertibility of the base regressor $\boldsymbol{Y}_b$. To do this the *condition number* of $\boldsymbol{Y}_b$ is found. The second measure is the error between the measured wrench, and the wrench predicted by the recovered parameters:

$$\epsilon=\|\boldsymbol{\Gamma}_T-\boldsymbol{Y}_b\boldsymbol{\psi}\|_2 \tag{5}$$

where $\boldsymbol{\Gamma}_T$ is the net effect of the contact wrenches. If the condition number and error ϵ are low, the parameters recovered via inverting Equation 4 are taken to be accurate.

These base parameters are then typically used to deduce the full set of dynamic parameters, via optimisation or modelling approaches [8][9].

B. Geometric Robotics

Geometric robotics represents operations such as rotations and homogeneous transforms as elements in mathematical groups [10].

1) Lie Groups and Algebras: The set of all rotations $\boldsymbol{R}$ can be written as the set of Special Orthogonal matrices $SO(3)$ where:

$$SO(3)=\left\{\boldsymbol{R}\in\mathbb{R}^{3\times3}\middle|\boldsymbol{R}\boldsymbol{R}^T=\mathbb{I},det(\boldsymbol{R})=1\right\}$$

$SO(3)$ is a group, specifically a Lie Group [6].

Every Lie group has a corresponding Lie Algebra. The Lie algebra associated with $SO(3)$ is $\mathfrak{so}(3)$, the space of skew-symmetric matrices:

$$\mathfrak{so}(3)=\left\{\boldsymbol{S}\in\mathbb{R}^{3\times3}\middle|\boldsymbol{S}^T=-\boldsymbol{S}\right\}$$

The exponential map exp maps the Lie Algebra to the Lie Group. Given a rotation axis $\boldsymbol{\omega}$, and a rotation angle θ, the corresponding rotation can therefore be found via:

$$\boldsymbol{R}=exp\left(\hat{\boldsymbol{\omega}}\theta\right)$$

where $\hat{\boldsymbol{\omega}}$ is the matrix form of the cross product by $\boldsymbol{\omega}$:

$$\hat{\boldsymbol{\omega}}=\begin{bmatrix}0&-\omega_3&\omega_2\\ \omega_3&0&-\omega_1\\ -\omega_2&\omega_1&0\end{bmatrix}$$

(note $\hat{\boldsymbol{\omega}}\boldsymbol{b}=\boldsymbol{\omega}\times\boldsymbol{b}$)

The utility of this form is that given any axis of rotation $\boldsymbol{\omega}$, and the angle to rotate about it, the full rotation matrix $\boldsymbol{R}$ can be computed (Rodrigues formula) [10].

This result can be extended to full rigid body motion by looking at the Special Euclidean group $SE(3)$, with the corresponding Lie algebra:

$$\mathfrak{se}(3)=\left\{(\boldsymbol{v},\hat{\boldsymbol{\omega}})\middle|\boldsymbol{v}\in\mathbb{R}^3,\hat{\boldsymbol{\omega}}\in\mathfrak{so}(3)\right\}$$

The pair of linear and rotational velocities $(\boldsymbol{v},\hat{\boldsymbol{\omega}})$ can be represented by the twist $\boldsymbol{\xi}$ and the wedge operator where:

$$\hat{\boldsymbol{\xi}}=\widehat{\begin{bmatrix}\boldsymbol{v}\\ \boldsymbol{\omega}\end{bmatrix}}=\begin{bmatrix}\hat{\boldsymbol{\omega}}&\boldsymbol{v}\\ \mathbb{O}&0\end{bmatrix}$$

As with rotations, any homogeneous rigid body transformation can be written in exponential form:

$$\boldsymbol{g}=exp\left(\hat{\boldsymbol{\xi}}\theta\right)$$

2) Velocities: The velocities of a system can be written in two forms: spatial $\boldsymbol{V}^s$, and body $\boldsymbol{V}^b$ depending on the frame of reference:

$$\boldsymbol{V}^s_{ab}=\dot{\boldsymbol{g}}_{ab}(\theta)\boldsymbol{g}^{-1}_{ab}(\theta)\quad \boldsymbol{V}^b_{ab}=\boldsymbol{g}^{-1}_{ab}(\theta)\dot{\boldsymbol{g}}_{ab}(\theta)$$

These two velocities are linked by the *adjoint* relation [10]:

$$\begin{gathered}\boldsymbol{V}^s=Ad_{\boldsymbol{g}}\boldsymbol{V}^b\\ \boldsymbol{V}^s_{a,c}=\boldsymbol{V}^s_{a,b}+Ad_{\boldsymbol{g}_{a,b}}\boldsymbol{V}^s_{b,c}\\ \boldsymbol{V}^b_{a,c}=Ad_{\boldsymbol{g}^{-1}_{b,c}}\boldsymbol{V}^b_{a,b}+\boldsymbol{V}^b_{b,c}\end{gathered} \tag{6}$$

with:

$$Ad_{\boldsymbol{g}}=\begin{bmatrix}\boldsymbol{R}&\hat{\boldsymbol{p}}\boldsymbol{R}\\ \mathbb{O}&\boldsymbol{R}\end{bmatrix},\quad ad_{\boldsymbol{g}}=\begin{bmatrix}\hat{\boldsymbol{\omega}}&\hat{\boldsymbol{v}}\\ \mathbb{O}&\hat{\boldsymbol{\omega}}\end{bmatrix}$$

IV. FORMULATION

A. Recursion Form of Newton-Euler

Recursive formulae for modelling system dynamics can be written geometrically [11]. These formulae act as an algorithmic approach for computing the kinematics (forward), and inverse dynamics (backwards). To derive the recursive forms, two relations are introduced:

$$\begin{gathered}\boldsymbol{g}_i = \boldsymbol{g}_{i-1}\boldsymbol{g}_{i-1,i} \\ \boldsymbol{g}_{i-1,i} = \boldsymbol{g}_{i-1,i}(0)exp\left(\hat{\boldsymbol{\xi}}^{\ddagger}{}_i\theta_i\right)\end{gathered} \tag{7}$$

where:

$$\boldsymbol{\xi}_i^{\ddagger} = Ad_{\boldsymbol{g}_{i-1,i}^{-1}(0)}\boldsymbol{\xi}_i \tag{8}$$

These relations can be used to derive a recursive expression for the Newton-Euler dynamic equations using the geometric approach.

1) Forward Recursion ($i \geq 1$):

$$\begin{gathered}\boldsymbol{V}_0 = \mathbb{0}, \dot{\boldsymbol{V}}_0 = \left[\boldsymbol{g}^T, \mathbb{0}^T\right]^T \\ \boldsymbol{g}_{i-1,i} = \boldsymbol{g}_{i-1,i}(0)e^{\hat{\boldsymbol{\xi}}^{\ddagger}_{i-1,i}\dot{\theta}_i} \\ \boldsymbol{V}_i = Ad_{g_{i-1,i}^{-1}}\boldsymbol{V}_{i-1} + \boldsymbol{\xi}^{\ddagger}_{i-1,i}\dot{\theta}_i \\ \dot{\boldsymbol{V}}_i = Ad_{g_{i-1,i}^{-1}}\dot{\boldsymbol{V}}_{i-1} + \boldsymbol{\xi}^{\ddagger}_{i-1,i}\ddot{\theta}_i \\ - ad_{\xi^{\ddagger}_{i-1,i},\theta_i}\left(Ad_{\boldsymbol{g}_{i-1,i}^{-1}}V_{i-1}\right)\end{gathered} \tag{9}$$

where:

$$\begin{gathered}\boldsymbol{M}_i = \begin{bmatrix}\mathbb{I}m_i & -m_i\hat{r}_i \\ m_i\hat{r}_i & \boldsymbol{I}_i'\end{bmatrix} \\ \boldsymbol{I}_i' = \boldsymbol{I}_i - m_i\hat{r}_i^2\end{gathered} \tag{10}$$

2) Backward Recursion:

$$\begin{gathered}\boldsymbol{\Gamma}_i = Ad^T_{g_{i,i+1}^{-1}}\boldsymbol{\Gamma}_{i+1} + \boldsymbol{M}_i\dot{\boldsymbol{V}}_i - ad^T_{\boldsymbol{V}_i}\boldsymbol{M}_i\boldsymbol{V}_i \\ \boldsymbol{\tau}_{\boldsymbol{J}i} = \boldsymbol{\xi}_i^{\ddagger T}\boldsymbol{\Gamma}_i\end{gathered} \tag{11}$$

B. Dynamic Identification Modelling

Noting the structure of the backward recursion form (Equations 11), it is possible to develop a recursive expression for the *DIM*. As the dynamic parameters only appear in as the matrix products $\boldsymbol{M}_i\dot{\boldsymbol{V}}_i$ and $\boldsymbol{M}_i\boldsymbol{V}_i$, it is possible to rewrite these terms as two matrix products of the form $\boldsymbol{Y}_1\boldsymbol{\phi}$ and $\boldsymbol{Y}_2\boldsymbol{\phi}$. The local body velocity $\boldsymbol{V}_i^b$ can be decomposed into the two component velocities $\boldsymbol{\omega}_i^b$ and $\boldsymbol{v}_i^b$ giving the relation:

$$\begin{gathered}\boldsymbol{M}_i\boldsymbol{V}_i = \boldsymbol{Y}_{i,2}\boldsymbol{\phi}_i \\ \boldsymbol{Y}_{i,2} = \begin{bmatrix}\boldsymbol{v}_i^b & \hat{\boldsymbol{\omega}}_i^b & \mathbb{0} & \mathbb{0} \\ \mathbb{0} & -\hat{\boldsymbol{v}}_i^b & diag(\boldsymbol{\omega}_i^b) & \begin{matrix}\omega^b_{i,2} & \omega^b_{i,3} & 0 \\ \omega^b_{i,1} & 0 & \omega^b_{i,3} \\ 0 & \omega^b_{i,1} & \omega^b_{i,2}\end{matrix}\end{bmatrix}\end{gathered} \tag{12}$$

Obtaining a matrix of similar structure for $\boldsymbol{M}_i\dot{\boldsymbol{V}}_i$, the backwards recursion can be written as:

$$\begin{aligned}\boldsymbol{\Gamma}_i &= Ad^T_{g_{i,i+1}^{-1}}\boldsymbol{\Gamma}_{i+1} + \boldsymbol{M}_i\dot{\boldsymbol{V}}_i - ad^T_{\boldsymbol{V}_i}\boldsymbol{M}_i\boldsymbol{V}_i \\ &= Ad^T_{g_{i,i+1}^{-1}}\boldsymbol{\Gamma}_{i+1} + \boldsymbol{Y}_{i,1}\boldsymbol{\phi}_i - ad^T_{\boldsymbol{V}_i}\boldsymbol{Y}_{i,2}\boldsymbol{\phi}_i \\ &= Ad^T_{g_{i,i+1}^{-1}}\boldsymbol{\Gamma}_{i+1} + \left[\boldsymbol{Y}_{i,1} - ad^T_{\boldsymbol{V}_i}\boldsymbol{Y}_{i,2}\right]\boldsymbol{\phi}_i\end{aligned}$$

The recursive form of the geometric *DIM* is therefore:

$$\begin{gathered}\boldsymbol{\Gamma}_i = Ad^T_{g_{i,i+1}^{-1}}\boldsymbol{\Gamma}_{i+1} + \boldsymbol{Y}_i\boldsymbol{\phi}_i \\ \boldsymbol{Y}_i = \boldsymbol{Y}_{i,1} - ad^T_{\boldsymbol{V}_i}\boldsymbol{Y}_{i,2}\end{gathered} \tag{13}$$

Therefore, if the wrench at the base link $\boldsymbol{\Gamma}_0$ (the ground reaction force) is known, then the geometric DIM can be written in the standard DIM form:

$$\begin{gathered}\boldsymbol{\Gamma}_0 = \boldsymbol{Y}\boldsymbol{\phi} \\ \boldsymbol{Y} = \begin{bmatrix}\boldsymbol{Y}_0 & Ad^T_{g_{0,1}^{-1}}\boldsymbol{Y}_1 & \ldots & Ad^T_{g_{0,n}^{-1}}\boldsymbol{Y}_1\end{bmatrix} \\ \boldsymbol{\phi} = \begin{bmatrix}\boldsymbol{\phi}_0^T & \boldsymbol{\phi}_1^T & \ldots & \boldsymbol{\phi}_n^T\end{bmatrix}^T\end{gathered} \tag{14}$$

V. COMPUTATIONAL MODELLING

To verify the geometric DIM model, the resulting symbolic expression was compared to the DIM model obtained via OpenSYMORO [12]. OpenSYMORO is an open source symbolic modelling package used to model the dynamics of robotic systems, and can generate DIM regressors from a given modified DH table [5]. Several simple systems were modelled and compared including, both revolute and prismatic joints, and devices with multiple masses and degrees of freedom. In every case tested, the DIM models obtained from the DH and Geometric models were found to be identical. The formulation for a double pendulum system is shown below in both the DH and Geometric notations.

A. Double Pendulum

The first example is that of a vertical double pendulum mounted on a base (Figure 1). This model has two degrees of freedom, and three segments that have inertial parameters.

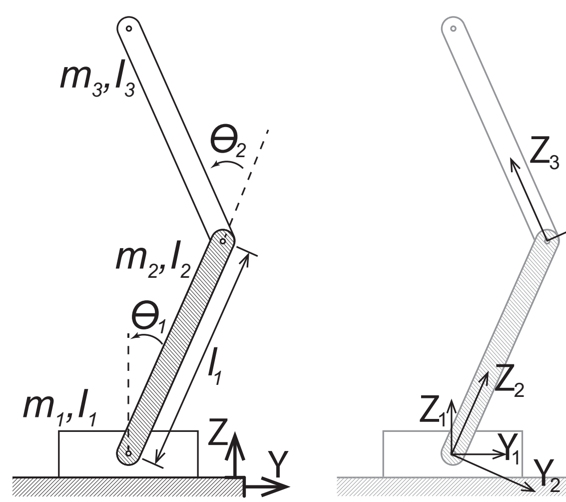

Fig. 1. Illustration of the double pendulum model. Left: Two links of mass and inertia m_2, I_3 and m_3, I_3 are attached to a rigid base m_1, I_1. The base is located at the coordinates $[T_x, T_y, T_z]^T$ with respect to the origin, and the rotations of the two links expressed by θ_1, θ_2. Right: The local coordinate frames for the base and two links.

1) DH Model: To match the system in Figure 1, it is required that the inertial coordinate frames of each body are simple translations of the world frame. Due to the DH convention only allowing for rotation/translation about/along the Z axis, a number of intermediary coordinate frames need to be added. Using the Modified Denavid-Hartenburg notation, we obtain the model found in Table I.

TABLE I

MODIFIED DH PARAMETERS FOR THE DOUBLE PENDULUM

DH Frame	1	2	3	4	5	6	7	8	9	10
Inertias	-	Base	-	-	-	Link 1	-	-	-	Link 2
α	$-\frac{\pi}{2}$	$\frac{\pi}{2}$	0	$-\frac{\pi}{2}$	$\frac{\pi}{2}$	0	0	$-\frac{\pi}{2}$	$\frac{\pi}{2}$	0
d	T_x	0	0	0	0	0	0	0	0	0
θ	0	0	$-\frac{\pi}{2}$	θ_1	0	$\frac{\pi}{2}$	$-\frac{\pi}{2}$	θ_2	0	$\frac{\pi}{2}$
r	T_y	T_z	0	0	0	0	l_1	0	0	0

2) Geometric Model: In contrast, the geometric model only requires the initial homogeneous pose for each link, and the twist of the joint. The geometric model for the double pendulum is shown in Table II.

TABLE II

GEOMETRIC MODEL FOR THE DOUBLE PENDULUM

Geometric Frame	Initial Pose $\boldsymbol{g}_{0,i}(0)$	Twist $\boldsymbol{\xi}^{\ddagger}_{i-1,i}$
Base, $i = 1$	$\begin{bmatrix} \mathbb{I} & \begin{matrix} T_x \\ T_y \\ T_z \end{matrix} \\ \mathbb{O} & 1 \end{bmatrix}$	$\begin{bmatrix} v_{0,1} \\ \omega_{0,1} \end{bmatrix} = \begin{bmatrix} \mathbb{O} \\ \mathbb{O} \end{bmatrix}$
Link 1, $i = 2$	$\begin{bmatrix} \mathbb{I} & \begin{matrix} T_x \\ T_y \\ T_z \end{matrix} \\ \mathbb{O} & 1 \end{bmatrix}$	$\begin{bmatrix} v_{1,2} \\ \omega_{1,2} \end{bmatrix} = \begin{bmatrix} \mathbb{O} \\ 1 \\ 0 \\ 0 \end{bmatrix}$
Link 2, $i = 3$	$\begin{bmatrix} \mathbb{I} & \begin{matrix} T_x \\ T_y \\ T_z + l_1 \end{matrix} \\ \mathbb{O} & 1 \end{bmatrix}$	$\begin{bmatrix} v_{2,3} \\ \omega_{2,3} \end{bmatrix} = \begin{bmatrix} \mathbb{O} \\ 1 \\ 0 \\ 0 \end{bmatrix}$

VI. MISALIGNED ROTATIONS

When estimating the dynamic parameters of a structure, the kinematic model used for dynamic recovery are frequently simplified. This is due to the complexity of writing the rotation about an arbitrary axis in DH form. Section V showed that a representative DIM model can be generated using a geometric approach. This section shows the importance of fully modelling axis of rotation when computing the DIM.

To compare the effects that these small changes in axis have on the dynamic parameter recovery, the errors in the estimated base parameters are shown. It is important to note that the parameter regroupings may differ between the two models. As such, the true inertial parameters $\boldsymbol{\phi}_T$ are used to calculate the expected value for the regrouped base parameters $\boldsymbol{\psi}_{T,Full}$, $\boldsymbol{\psi}_{T,Simple}$ for the full and simplified models respectively. By finding the percentage error between the recovered base parameters and the true base parameters, it is possible to compare the accuracy of these two modelling approaches.

A. Double Pendulum

The double pendulum system example is examined, now accounting for potential inaccuracies in the mounting and manufacture of the two revolute joints. Instead of only rotating about the X axis, the joints rotate about an axis 5^o offset from the X axis. The effect of neglecting this variation in axis is then investigated.

Through parameter identification methods, it is possible to recover the true axis of rotation given kinematic data. This kinematic model is then used to generate two DIM representations. The first is model simplifies the axis of rotation, aligning it to the Euclidian X axis (a typical simplification used in DH DIM modelling). The second model is generated via the presented geometric form. The true axes of rotation are easily implementable by updating $\boldsymbol{\xi}^{\ddagger}_{1,2}$ and $\boldsymbol{\xi}^{\ddagger}_{2,3}$ to match the recovered axes of rotation. This is found by updating $\boldsymbol{\omega}_{1,2}$, $\boldsymbol{\omega}_{2,3}$ to lie along the true axes [13].

The system was excited with noisy acceleration sinusoids which were then integrated to obtain velocity and position trajectories. The kinematic and dynamic data was based on a UR5 robot. The condition numbers for the simplified and full regressors were both found to be 38.1 ($\boldsymbol{Y} \in \mathbb{R}^{4715\times13}$). and 334.2 ($\boldsymbol{Y} \in \mathbb{R}^{5658\times13}$.) respectivley. The recovered base parameters are shown in Table III, with the error in the recovered wrenches plotted in Figure 2. Note that some of the true values are omitted due to the different form during the regrouping process.

TABLE III

MINIMAL PARAMETERS AND THEIR RELATIVE ERRORS

Parameter	Simplified Model Error	Full Model Error
$(m_1)_R$	0.00	0.00
$(m_1 r_{x,1})_R$	0.32	$\mathbf{-0.11}$
$(m_1 r_{y,1})_R$	-0.03	**0.00**
$m_2 r_{y,2}$	$\mathbf{-0.06}$	0.14
$(m_2 r_{z,2})_R$	0.06	**0.02**
$(I_{xx,2})_R$	0.04	**0.02**
$I_{xy,2}$	-1.17	**0.13**
$(I_{xz,2})_R$	-2.15	**0.15**
$m_3 r_{y_3}$	-0.09	**0.02**
$m_3 r_{z_3}$	-0.10	**0.00**
$I_{xx,3}$	0.04	**0.03**
$I_{xy,3}$	-0.42	$\mathbf{-0.10}$
$I_{xz,3}$	-0.55	**0.16**

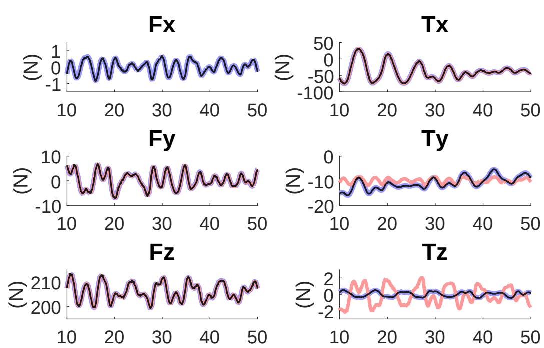

Fig. 2. Recovered wrench for DH recovery (red) and Geometric recovery (blue) plotted against the true wrench (black). X axis shows time, Y axis shows the magnitude of the wrench component.

B. Discussion

Table III compares the errors in the recovered base parameters between the two different modelling forms. The error values are computed from comparing the recovered values, to the values computed from the true dynamic parameters and the corresponding regrouping equations. The Table shows significant errors arise in the recovered dynamic parameters when small variations in the rotational axis are neglected. Of these, the most notable are the off axis inertias: I_{xy}, I_{xz}. These inertias appear due to the simplified DH model attempting to fit the out-of-plane forces and torques.

It is important to note that while there are significant errors in the recovered base parameters, these errors are not immediately obvious. The condition number for full model are larger than for the simplified model. This due to the condition number acting as a metric on invertability of the regressor, rather than acting as a measure of how valid the regressor and model is. As the regressor for the full model is larger simply comparing the two condition numbers is not sufficient to determine the accuracy of the recovered parameters.

The errors in the contact wrench also initially appear reasonable (Figures 2, 3). Care should therefore be taken when performing dynamic identification as modelling simplifications produced significant errors in recovered parameters, while appearing to be consistent with the data.

The full model accounts for the true rotation axis. The errors in the recovered parameters and the recovered wrenches are far lower than in the simplified model. While it is possible to generate the full model via the DH approach, it involves numerous intermediate frames potentially causing errors during implementation. In contrast, the geometric form is far simpler to implement as only the rotation axes $\boldsymbol{\omega}_{1,2}$, $\boldsymbol{\omega}_{2,3}$ need to be updated. Geometric tools therefore act as a method for generating DIM models where the axis of rotation can be written explicitly, resulting in improved dynamic parameter recovery.

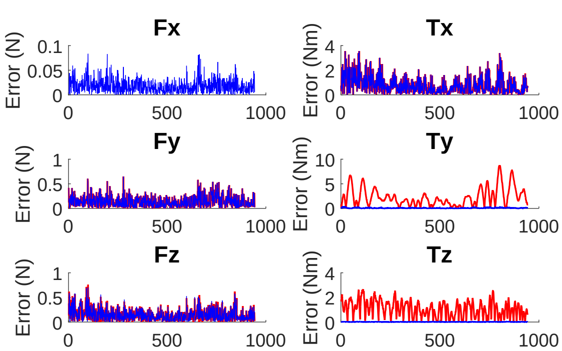

Fig. 3. Absolute error in recovered wrench for DH recovery (red) and Geometric recovery (blue). X axis shows sample number, Y axis shows the error between the recovered wrench and the true wrench (without noise).

VII. MULTIPLE CONTACTS

The dynamic identification process may require multiple points of contact. This situation may arise in cases where the system requires external support to perform exciting trajectories. In these cases, a model that allows for arbitrary interaction wrenches is required. These arbitrary wrenches can be easily accounted for by exploiting the separable structure of the recursive geometric DIM (Equation 13).

Consider an arbitrary external wrench exerted on link i ($\boldsymbol{\Gamma}_{E,i}$). The total wrench on link i can then be written:

$$\boldsymbol{\Gamma}_i = Ad^T_{g^{-1}_{i,i+1}} \boldsymbol{\Gamma}_{i+1} + \boldsymbol{Y}_i \boldsymbol{\phi}_i + \boldsymbol{\Gamma}_{E,i} \tag{15}$$

This wrench can be expressed in the base frame by Equation 16.

$$\begin{aligned}
\boldsymbol{\Gamma}_{0,i} &= Ad^T_{g^{-1}_{0,1}} \left(Ad^T_{g^{-1}_{1,2}} \dots Ad^T_{g^{-1}_{i,i+1}} \left(\boldsymbol{\Gamma}_i\right)\right) \\
\boldsymbol{\Gamma}_{0,i} &= Ad^T_{g^{-1}_{0,i}} \left(Ad^T_{g^{-1}_{i,i+1}} \boldsymbol{\Gamma}_{i+1} + \boldsymbol{Y}_i \boldsymbol{\phi}_i + \boldsymbol{\Gamma}_{E,i}\right) \\
\boldsymbol{\Gamma}_{0,i} &= Ad^T_{g^{-1}_{0,i}} \left(Ad^T_{g^{-1}_{i,i+1}} \boldsymbol{\Gamma}_{i+1} + \boldsymbol{Y}_i \boldsymbol{\phi}_i \right) + Ad^T_{g^{-1}_{0,i}} \left(\boldsymbol{\Gamma}_{E,i}\right)
\end{aligned} \tag{16}$$

Given the external wrenches ($\boldsymbol{\Gamma}_{E,i}$) measured at each contact point, the total measured wrench of the system in the base frame can be written as:

$$\boldsymbol{\Gamma}_T = \boldsymbol{\Gamma}_0 - \sum_{i=1}^{N_c} Ad_{g^{-1}_{0,i}} \left(\boldsymbol{\Gamma}_{E,i}\right) \tag{17}$$

The full geometric DIM model for multiple contacts can therefore be written as:

$$\begin{gathered}
\boldsymbol{\Gamma} = \boldsymbol{Y}\boldsymbol{\phi} \\
\boldsymbol{\Gamma} = \boldsymbol{\Gamma}_0 - \textstyle\sum_{i=1}^{N_c} Ad^T_{g^{-1}_{0,i}} \left(\boldsymbol{\Gamma}_{E,i}\right) \\
\boldsymbol{Y} = \begin{bmatrix} \boldsymbol{Y}_0 & Ad^T_{g^{-1}_{0,1}} \boldsymbol{Y}_1 & \dots & Ad^T_{g^{-1}_{0,n}} \boldsymbol{Y}_1 \end{bmatrix} \\
\boldsymbol{\phi} = \begin{bmatrix} \boldsymbol{\phi}_0^T & \boldsymbol{\phi}_1^T & \dots & \boldsymbol{\phi}_n^T \end{bmatrix}^T
\end{gathered} \tag{18}$$

A. Double Pendulum

To investigate the effect multiple contact points have on the dynamic identification process, the double pendulum system is again examined. The double pendulum is now modelled as having two contact wrenches, the contact wrench with the ground, and a new contact wrench acting at the end of the second link. The system was driven through a range of joint angles, and wrenches at the second link ($\boldsymbol{\Gamma}_{E,2}$). The corresponding contact wrench at the base $\boldsymbol{\Gamma}_0$ was then determined.

From this simulation, noise was introduced to the joint states and contact wrenches. This produced the simulated states ($\boldsymbol{\theta}$, $\dot{\boldsymbol{\theta}}$ and $\ddot{\boldsymbol{\theta}}$), and the regressor $\boldsymbol{Y}$ found. Given this simulated dataset, the condition number was found to be 36.5 for $\boldsymbol{Y} \in \mathbb{R}^{4715\times 13}$. The measured total effective wrench $\boldsymbol{\Gamma}$ was found from $\boldsymbol{\Gamma}_0$ and $\boldsymbol{\Gamma}_{E,2}$. Equation 18 was then used to recover the base inertial parameters $\boldsymbol{\phi}$ (Table III). The measured ground wrench, computed total effective wrench, and the predicted wrench using the recovered $\boldsymbol{\psi}$ are shown in Figure 4, with the error shown in Figure 5.

B. Discussion

Table IV shows the recovered base parameters for the multi contact double pendulum system. While the relation between the two contact wrenches can be complex to model, the geometric wrench relation (Equation 17) is able to obtain net effect of these wrenches. As a result, the recovered dynamic parameters and wrenches were found reliably.

TABLE IV

MULTI-CONTACT DOUBLE PENDULUM: MINIMAL PARAMETERS

Parameter	True Value	Error
$(m_1)_R$	20.99	0.00
$(m_1 r_{x,1})_R$	1.33	0.00
$(m_1 r_{y,1})_R$	0.00	−0.01
$m_2 r_{y,2}$	0.00	0.00
$(m_2 r_{z,2})_R$	6.39	0.01
$(I_{xx,2})_R$	2.41	0.08
$I_{xy,2}$	0.00	−0.03
$(I_{xz,2})_R$	−0.56	0.01
$m_3 r_{y_3}$	0.00	0.00
$m_3 r_{z_3}$	2.66	0.00
$I_{xx,3}$	0.41	−0.01
$I_{xy,3}$	0.00	0.00
$I_{xz,3}$	0.00	0.00

The disparity in the wrenches can be seen clearly in Figure 4. In this system, the measured contact wrench $\mathbf{\Gamma}_0$ is plotted with the total effective wrench $\mathbf{\Gamma}$. It is therefore clear that the effect of the multiple contact points needs to be considered.

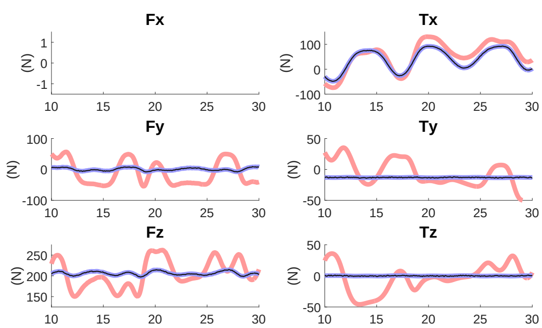

Fig. 4. Wrenches in the double multi-contact double pendulum model. Measured ground reaction wrench $\mathbf{\Gamma}_0$ is shown in red. The true total effective wrench $\mathbf{\Gamma}$ is shown in blue. The recovered wrench predicted from the recovered parameters is shown in black.

VIII. DISCUSSION

This work presents a geometric approach to dynamic parameter identification through contact measurement. Through the use of these geometric tools, it is possible to provide an accurate representation of the underlying structure of the system. As the axis of rotation can be written explicitly in the geometric form, accurate DIMs can be generated. Failure to model these differences may result in substantial errors in the recovered base parameters.

This work also presents an easily implementable form for dynamic identification in situations with multiple points of contact. By combining the multiple contact wrenches into a single effective wrench, the standard inverse dynamic modelling approaches can be used.

IX. FUTURE WORK

This work has introduced the mathematical formulation for computing dynamic parameters in multi-contact serial chain structures using geometric models. The investigation and validation of these methods have been restricted to pure simulation. The next step is to experimentally validate these methods on systems with known dynamic parameters to determine the reliability of these methods. One of the areas, multi-contact dynamic identification is the estimation of human mass segments in-vivo. This framework provides a basis for these assisted human modelling experiments.

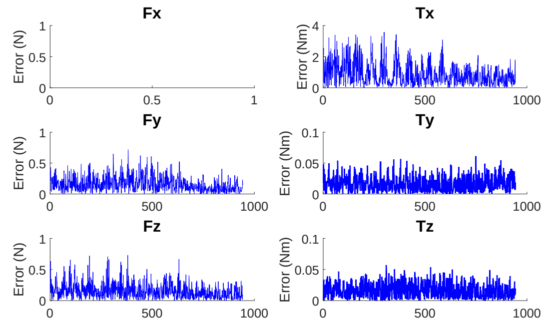

Fig. 5. The error between the measured wrench and the wrench predicted from the recovered parameters.

REFERENCES

[1] J. Wu, J. Wang, and Z. You, “An overview of dynamic parameter identification of robots,” *Robotics and computer-integrated manufacturing*, vol. 26, no. 5, pp. 414–419, 2010.

[2] P. K. Khosla and T. Kanade, “Parameter identification of robot dynamics,” in *Decision and Control, 1985 24th IEEE Conference on*. IEEE, 1985, pp. 1754–1760.

[3] K. Ayusawa, G. Venture, and Y. Nakamura, “Identification of humanoid robots dynamics using floating-base motion dynamics,” in *Intelligent Robots and Systems, 2008. IROS 2008. IEEE/RSJ International Conference on*. IEEE, 2008, pp. 2854–2859.

[4] G. Venture, K. Ayusawa, and Y. Nakamura, “Motion capture based identification of the human body inertial parameters,” in *Engineering in Medicine and Biology Society, 2008. EMBS 2008. 30th Annual International Conference of the IEEE*. IEEE, 2008, pp. 4575–4578.

[5] W. Khalil and E. Dombre, *Modeling, identification and control of robots*. Butterworth-Heinemann, 2004.

[6] J. Selig, *Geometrical methods in robotics*. Springer Science & Business Media, 2013.

[7] M. Gautier, “Dynamic identification of robots with power model,” in *Robotics and Automation, 1997. Proceedings., 1997 IEEE International Conference on*, vol. 3, Apr 1997, pp. 1922–1927 vol.3.

[8] K. Ayusawa, Y. Nakamura, and G. Venture, “Optimal estimation of human body segments dynamics using realtime visual feedback,” in *Intelligent Robots and Systems, 2009. IROS 2009. IEEE/RSJ International Conference on*. IEEE, 2009, pp. 1627–1632.

[9] M. Gautier and G. Venture, “Identification of standard dynamic parameters of robots with positive definite inertia matrix,” in *Intelligent Robots and Systems (IROS), 2013 IEEE/RSJ International Conference on*. IEEE, 2013, pp. 5815–5820.

[10] R. M. Murray, Z. Li, S. S. Sastry, and S. S. Sastry, *A mathematical introduction to robotic manipulation*. CRC press, 1994.

[11] F. C. Park, J. E. Bobrow, and S. R. Ploen, “A lie group formulation of robot dynamics,” *The International Journal of Robotics Research*, vol. 14, no. 6, pp. 609–618, 1995.

[12] W. Khalil, A. Vijayalingam, B. Khomutenko, I. Mukhanov, P. Lemoine, and G. Ecorchard, “Opensymoro: An open-source software package for symbolic modelling of robots,” in *Advanced Intelligent Mechatronics (AIM), 2014 IEEE/ASME International Conference on*. IEEE, 2014, pp. 1206–1211.

[13] A. Ude, C. Man, M. Riley, and C. G. Atkeson, “Automatic generation of kinematic models for the conversion of human motion capture data into humanoid robot motion,” in *in Proceedings of the First IEEE-RAS conference on Humanoid Robotics (Humanoids 2000), Massachusetts Institute of Technology*, 2000.